Acta Crystallographica Section F
Structural Biology and Crystallization Communications
ISSN 1744-3091

Purification, crystallization and preliminary X-ray diffraction of the G3BP1 NTF2-like domain

Tina Vognsen, Ingvar Rúnar Möller and Ole Kristensen*

Biostructural Research, Department of Medicinal Chemistry, Faculty of Pharmaceutical Sciences, University of Copenhagen, Universitetsparken 2, DK-2100 Copenhagen, Denmark

Correspondence e-mail: ok@farma.ku.dk

Received 14 June 2010
Accepted 17 October 2010

The nuclear transport factor 2-like (NTF2-like) domain of human G3BP1 was subcloned, overexpressed in *Escherichia coli* and purified. Crystals were obtained using the hanging-drop vapour-diffusion method. Diffraction data were collected to 3.6 Å resolution using synchrotron radiation. The crystals belonged to the hexagonal space group $P6_322$, with unit-cell parameters $a = b = 89.84$, $c = 70.02$ Å. The crystals contained one molecule per asymmetric unit, with an estimated solvent content of 56%. Initial phases were obtained by molecular replacement.

1. Introduction

Being overexpressed in breast-cancer tumours (French *et al.*, 2002), Ras-GTPase-activating protein SH3-domain-binding protein (G3BP) is considered to be a significant cancer marker protein. It was identified in a screen for proteins binding to the SH3 domain of Ras-GTPase-activating protein (RasGAP; Parker *et al.*, 1996). Initially, multiple P*xx*P motifs found in a proline-rich region of the protein were thought to be responsible for binding to the RasGAP SH3 domain (Parker *et al.*, 1996), but the binding site was subsequently located to the N-terminal nuclear transport factor 2-like (NTF2-like) domain of G3BP (Kennedy *et al.*, 2002). Besides binding to RasGAP, G3BP manages multiple tasks: it takes part in c-myc mRNA turnover (Gallouzi *et al.*, 1998), interacts with ubiquitin-specific proteases (Soncini *et al.*, 2001) and is involved in NF-κB regulation (Prigent *et al.*, 2000) and stress granule assembly (Tourrière *et al.*, 2003).

Binding to RasGAP takes place only when Ras p21, a protein involved in cell proliferation, is in its active GTP-binding state where cell division is induced (Parker *et al.*, 1996). It has been hypothesized that RasGAP–G3BP complex formation detrimentally prevents inactivation of Ras p21 in proliferating cells (Parker *et al.*, 1996).

Human G3BP exists in two variants, G3BP1 and G3BP2, located on chromosomes 5 and 4, respectively, and G3BP2 is found in two splice isoforms, G3BP2a and G3BP2b (Kennedy *et al.*, 2002). The full-length G3BP1 and G3BP2a proteins contain 466 and 482 residues, respectively, and have a sequence identity of 65%. In addition to the NTF2-like domain, G3BP also contains an RNA-binding domain and glutamate-rich and glycine-rich regions, and the central part of the protein contains multiple P*xx*P motifs. The main differences between the G3BP variants are found in the number of P*xx*P motifs.

The NTF2-like domain of human G3BP1 is comprised of 123 highly conserved amino acids (residues 11–133) and has a calculated molecular weight of 14 kDa. Recently, a molecular model of the NTF2-like domain of G3BP in complex with the RasGAP SH3 domain has been published (Cui *et al.*, 2010). Cui and coworkers based their model on a combination of homology modelling, protein–protein docking and molecular-dynamics simulations. However, obtaining an experimental structure of the NTF2-like domain is important in order to increase the reliability of molecular-modelling attempts and to investigate the potential of G3BP as a drug target.

Here, we report the expression, purification, crystallization and preliminary X-ray diffraction results of the human G3BP1 NTF2-like domain.

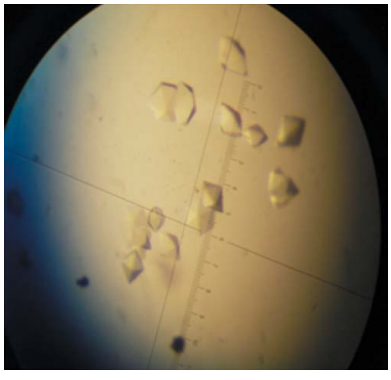

2. Experimental procedures

2.1. Subcloning

An expression plasmid was constructed by the polymerase chain reaction (PCR); template cDNA coding for human G3BP1 (Swiss-Prot Q13283) was kindly provided by B. Moss (Katsafanas & Moss, 2004) and DNA-fragment amplification was achieved using two primers containing designed restriction sites (hNTF2.G3BP1-F, 5′-CGCGGCAGCATATGGTCGGGCGGGAATTTGTGAGA-3′, and hNTF2.G3BP1-R, 5′-CGCGGCAGGCGGCCGCTCAACCAAAG-ACCTCATCTTGG-3′). The PCR product was digested with *Nde*I and *Not*I and cloned into the expression vector pET28a(+) (Novagen) by conventional ligation-dependent cloning. This construct contained a thrombin-cleavable N-terminal His_6 tag fused to the coding sequence of the NTF2-like domain (G3BP1 residues 11–139), leaving four additional vector-derived N-terminal residues after proteolysis (GSHM). The recombinant vector containing the target gene was verified by DNA sequencing (Eurofins MWG Operon).

2.2. Expression and purification

The plasmid was transformed into competent *Escherichia coli* BL21 (DE3) cells and grown at 310 K overnight on LB agar containing 30 µg ml^{-1} kanamycin. 30 ml LB medium was inoculated with a single colony from the LB agar plate and grown at 310 K to an OD_{600} of 0.6. 5 ml preculture was transferred to 1 l ZYM-5052 autoinduction medium (Studier, 2005), grown at 310 K for 4 h and then incubated at 303 K overnight. Cells were harvested by centrifugation at 277 K and resuspended on ice in phosphate-buffered saline containing 20 µg ml^{-1} RNase A, 20 µg ml^{-1} DNase I and EDTA-free protease-inhibitor cocktail tablets (Roche). Lysis was achieved by mechanical force in a cell disrupter operated at 190 MPa and 277 K (Constant Systems Ltd). The lysate was centrifuged at 43 146*g* and 277 K for 30 min and subsequently at 71 171*g* and 277 K for 30 min.

The supernatant was loaded onto a 5 ml HisTrap HP column (GE Healthcare) equilibrated with buffer *A* (20 m*M* Na_2HPO_4 pH 8, 30 m*M* imidazole, 300 m*M* NaCl). The column was washed with five column volumes (CV) of buffer *A* and the protein was eluted at room temperature with a linear gradient from 0 to 20% buffer *B* (20 m*M* Na_2HPO_4 pH 8, 1 *M* imidazole, 300 m*M* NaCl) over 5 CV followed by 20–100% buffer *B* over 10 CV. Fractions containing the target protein were collected and the following were added: $CaCl_2$ to a final concentration of 0.5 m*M*, 0.1%(*v*/*v*) β-mercaptoethanol and 2 U thrombin (bovine, Calbiochem) per milligram of protein. The mixture was left at room temperature and checked daily on SDS–PAGE to verify His_6-tag removal. A Superdex 75 (GE Healthcare) chromatography column equilibrated with GF buffer (10 m*M* Tris–HCl pH 8, 100 m*M* NaCl) at room temperature was used for the final purification and the protein was concentrated by ultrafiltration (Amicon Ultracel 10K). Protein concentrations were estimated using the Bradford protein assay (Bio-Rad).

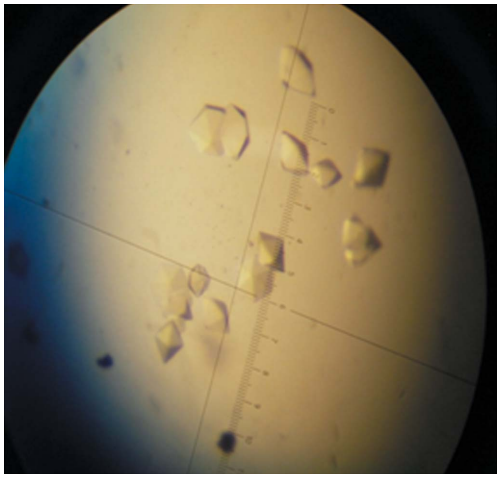

Figure 1
Hexagonal crystals of the G3BP1 NTF2-like domain. The crystals appeared in 1.6 *M* diammonium hydrogen phosphate, 0.1 *M* MOPS pH 8 and grew to dimensions of 0.2 × 0.2 × 0.15 mm in 1 d.

2.3. Protein crystallization

Initial crystallization conditions were found using a published method for high-throughput crystallization (Luft *et al.*, 2003). Crystals were obtained in six out of 1536 experiments and the most promising conditions were adapted for hanging-drop vapour-diffusion experiments at 293 K; crystals were obtained by mixing 2 µl protein solution (10 mg ml^{-1}) and 2 µl reservoir solution (1.6 *M* diammonium hydrogen phosphate, 0.1 *M* MOPS pH 8). The crystal used for the reported data collection was obtained under these standard conditions. The crystal was soaked in a solution consisting of 2 m*M* $HgCl_2$ and 1.6 *M* sodium/potassium phosphate buffer pH 7 and was incubated for 3 h before crystal harvesting. The Silver Bullets screen (Hampton Research) was used in cocrystallization experiments to investigate crystal optimization possibilities by mixing 2 µl protein solution (10 mg ml^{-1}) with 1 µl reservoir solution (1.6 *M* diammonium hydrogen phosphate, 0.1 *M* MOPS pH 8) and 1 µl Silver Bullets additive solution.

2.4. Data collection

The crystal used for data collection was flash-cooled after a brief soak in 1.6 *M* sodium/potassium phosphate pH 7 and 20% glycerol. Data were collected at 100 K on beamline ID14-1 at the European Synchrotron Radiation Facility (ESRF) equipped with an ADSC Q210 CCD detector and on beamline I911-2 at MAX-lab (Lund, Sweden) equipped with a MAR165 detector. Data processing was carried out using *XDS* (Kabsch, 2010) as implemented in the *xia*2 software (Winter, 2010). Matthews coefficient and solvent-content estimations were performed using the *CCP*4 software (Collaborative Computational Project, Number 4, 1994) and heavy-atom derivative analysis was performed using *SHELXC*/*D*/*E* (Sheldrick, 2008) in the *HKL2MAP* interface (Pape & Schneider, 2004). The *BALBES* (Long *et al.*, 2008) and *Phaser* (McCoy *et al.*, 2007) programs were used for molecular-replacement analysis.

3. Results and discussion

Human G3BP1 (residues 11–139) was successfully subcloned and overexpressed in *E. coli*. The protein eluted as a single peak in size-exclusion chromatography at a position that indicated dimerization of the G3BP1 NTF2-like domain. The protein contains a single cysteine residue, but dimer formation was observed to be independent of the presence or absence of reducing agents in the buffer (data not shown). The protein was more than 95% pure as judged by SDS–PAGE.

Hexagonal-shaped crystals appeared in the hanging-drop experiments within 1 d and several conditions from the Silver Bullets screen supported crystal growth (see Fig. 1). All crystals tested diffracted to 7 Å resolution or better when flash-cooled at 100 K with 20% glycerol as a cryoprotectant and several complete data sets were

Table 1
Data-collection statistics.

Values in parentheses are for the outer shell.

Beamline	MAX-lab I911-2
Wavelength (Å)	1.04
Space group	$P6_322$
Unit-cell parameters (Å, °)	$a = b = 89.84$, $c = 70.02$, $\alpha = \beta = 90$, $\gamma = 120$
Resolution range	27.11–3.59 (3.68–3.59)
No. of unique reflections	2129 (158)
Completeness (%)	98.0 (99.3)
Multiplicity	9.8 (10.2)
$\langle I/\sigma(I)\rangle$	17.6 (4.6)
$R_{\rm merge}$	0.081 (0.563)
$R_{\rm p.i.m.}$	0.028 (0.189)

collected at resolutions of around 4 Å. Crystals mounted in capillaries and tested at room temperature (data not shown) showed diffraction to 2.8 Å resolution using synchrotron radiation (MAX-lab, beamline I911-3), but suffered from severe radiation damage. Significant diffraction decay was observed within 3° of rotation when crystals were exposed to standard synchrotron X-ray doses at room temperature. Despite the favourable point-group symmetry of the crystals, it would most likely not be a trivial task to obtain a complete room-temperature data set by merging the data from several crystals. No systematic increase in diffraction potential or tolerance towards cryoprotection was observed from crystals grown using Silver Bullets additives, indicating that the intended stabilization of crystal contacts was not achieved. Data-collection and processing statistics for the best data set are shown in Table 1. A conservative resolution cutoff has been applied since the diffraction deteriorates rapidly beyond 3.6 Å resolution. The crystals belonged to space group $P6_322$, with unit-cell parameters $a = b = 89.84$, $c = 70.02$ Å, $\alpha = \beta = 90$, $\gamma = 120°$. The Matthews coefficient was calculated as 2.56 Å^3 Da^{-1}, corresponding to one molecule per asymmetric unit and an estimated solvent content of 56%. Despite the crystal having been soaked in $HgCl_2$ before data collection, no significant anomalous scattering corresponding to heavy-atom binding was observed. Initial phases were obtained by the molecular-replacement (MR) method with automatic search-model selection in the *BALBES* program. The *Cryptosporidium parvum* nuclear transport factor 2 (PDB entry 1zo2, chain *A*; Vedadi *et al.*, 2007), which has 31% similarity to the target sequence, provided a possible MR solution with $R_{\rm work}$ and $R_{\rm free}$ values of 35% and 45%, respectively. The correctness of this solution and the space-group assignment were verified by the program *Phaser*, which reported a final *Z* score of 21.1, a positive log-likelihood gain and no conflicting crystal-packing clashes of the model. An electron-density map was calculated which indicated that overall the model was both suitable and correctly placed in the unit cell. Packing of the molecular-replacement model supported the expected dimer formation. The single cysteine residue in the protein appears to be partially accessible and lack of derivatization by $HgCl_2$ soaking could be a consequence of too short an incubation time. To aid model building and refinement, efforts will be continued to obtain higher resolution diffraction.

We appreciate the support during data collection from the staff at ESRF, Grenoble (beamline ID14-1) and MAX-lab, Lund (beamline I911-2). Initial crystallization studies were performed by Dr B. Ross. This work was supported by the Lundbeck Foundation (OK; grant 244/06), the Danish Natural Science Council through DANSCATT and by a University of Copenhagen PhD fellowship (TV).

References

Collaborative Computational Project, Number 4 (1994). *Acta Cryst.* D**50**, 760–763.
Cui, W., Wei, Z., Chen, Q., Cheng, Y., Geng, L., Zhang, J., Chen, J., Hou, T. & Ji, M. (2010). *J. Chem. Inf. Model.* **50**, 380–387.
French, J., Stirling, R., Walsh, M. & Kennedy, H. D. (2002). *Histochem. J.* **34**, 223–231.
Gallouzi, I., Parker, F., Chebli, K., Maurier, F., Labourier, E., Barlat, I., Capony, J. P., Tocque, B. & Tazi, J. (1998). *Mol. Cell. Biol.* **18**, 3956–3965.
Kabsch, W. (2010). *Acta Cryst.* D**66**, 125–132.
Katsafanas, G. C. & Moss, B. (2004). *J. Biol. Chem.* **279**, 52210–52217.
Kennedy, D., French, J., Guitard, E., Ru, K., Tocque, B. & Mattick, J. (2002). *J. Cell. Biochem.* **84**, 173–187.
Long, F., Vagin, A. A., Young, P. & Murshudov, G. N. (2008). *Acta Cryst.* D**64**, 125–132.
Luft, J. R., Collins, R. J., Fehrman, N. A., Lauricella, A. M., Veatch, C. K. & DeTitta, G. T. (2003). *J. Struct. Biol.* **142**, 170–179.
McCoy, A. J., Grosse-Kunstleve, R. W., Adams, P. D., Winn, M. D., Storoni, L. C. & Read, R. J. (2007). *J. Appl. Cryst.* **40**, 658–674.
Pape, T. & Schneider, T. R. (2004). *J. Appl. Cryst.* **37**, 843–844.
Parker, F., Maurier, F., Delumeau, I., Duchesne, M., Faucher, D., Debussche, L., Schweighofer, F. & Tocque, B. (1996). *Mol. Cell. Biol.* **16**, 2561–2569.
Prigent, M., Barlat, I., Langen, H. & Dargemont, C. (2000). *J. Biol. Chem.* **275**, 36441–36449.
Sheldrick, G. M. (2008). *Acta Cryst.* A**64**, 112–122.
Soncini, C., Berdo, I. & Draetta, G. (2001). *Oncogene*, **20**, 3869–3879.
Studier, F. W. (2005). *Protein Expr. Purif.* **41**, 207–234.
Tourrière, H., Chebli, K., Zekri, L., Courselaud, B., Blanchard, J. M., Bertrand, E. & Tazi, J. (2003). *J. Cell Biol.* **160**, 823–831.
Vedadi, M. *et al.* (2007). *Mol. Biochem. Parasitol.* **151**, 100–110.
Winter, G. (2010). *J. Appl. Cryst.* **43**, 186–190.